Renormalized Resonance Frequencies of a Ferrite Sphere Coupled to an LR Circuit: Comparison of Theory and Experiment

L.Q. ENGLISH, C. KERESTES, G. RYDZAG

Department of Physics and Astronomy, Dickinson College, Carlisle, Pennsylvania 17013

ABSTRACT: We derive a formula for the AC susceptibility of a ferrite spherical resonator coupled to an LR circuit by formulating the problem in terms of a feedback mechanism. This technique allows us to find an analytical expression for the dependence of the shift in resonance frequency on the loop-crystal coupling strength, the circuit parameters, and the saturation magnetization of the ferrite. Finally, we compare these predictions to experimental results on YIG and Ga:YIG spheres. This coupling provides a simple way of tuning the uniform mode frequency relative to the spin-wave spectrum. Concepts Magn Reson Part B (Magn Reson Engineering) 24B: 39–45, 2005

KEY WORDS: ferromagnetic resonance; dynamic susceptibility; YIG spheres; magnetostatic modes; coupling to magnetic resonance; frequency renormalization; microwave coupling structures; magnetic feedback

INTRODUCTION

Yttrium iron garnet (YIG) is a ferromagnetic insulator with a large room-temperature saturation magnetization and a sharp ferromagnetic resonance. These properties make it ideal in many microwave applications. Over the last half-century, YIG and other ferrites have played a crucial role in communications systems and microwave engineering; they are the central component in everything from wideband tunable microwave filters and oscillators to nonreciprocal devices, such as circulators, isolators, and phase shifters (*1, 2*).

YIG has also been of much interest from a fundamental science perspective. In the late 1950s, it was one of the early materials in which nonuniform magnetic resonance was observed, and it was thus instrumental in the development of the theory of magnetostatic modes (*3, 4*). Around the same time, it served as a convenient experimental system for the study of nonlinear processes and instabilities in magnetic systems (*5*). More recently, thin films of YIG have proved ideal for the generation and detailed study of envelope solitons (*6*).

It has long been known that the resonance frequency and effective Q-factor of a cavity change when a ferrite is placed in it (*1, 7–9*). Analytical expressions for such shifts in the resonance frequency of a microwave cavity can be derived using a cavity perturbation approach. In that problem, one finds that many experimental factors influence the shift, such as electric and magnetic field magnitude and configuration in the cavity, the position of the sample in the cavity, and external coupling to the cavity (*8, 9*).

Here we present another look at the well-studied problem of external coupling to the ferromagnetic resonance of a ferrite. Instead of treating the cavity problem, we examine the coupling of a ferrite sample to a nonresonant loop antenna and derive an exact relationship without recourse to a perturbative

Received 1 September 2004; accepted 18 October 2004

Correspondence to: L.Q. English; E-mail: englishl@dickinson.edu

Concepts in Magnetic Resonance Part B (Magnetic Resonance Engineering), Vol. 24B(1) 39–45 (2005)

Published online in Wiley InterScience (www.interscience.wiley.com). DOI 10.1002/cmr.b.20026

method. In the past, the analysis of this problem was formulated within the framework of scattering theory. Consequently, that work focused on the calculation of scattering parameters and impedances in microwave networks, which included ferrite components (*1, 10, 11*). In this study we develop an alternative, more direct approach to the coupled ferromagnetic resonance problem for a specific geometry by mapping it to a feedback diagram. This formulation of the problem in terms of a feedback mechanism, which should be easily accessible to advanced undergraduates, allows us to compute coupled AC susceptibility curves and to quantify the phenomenon of frequency renormalization. These results are then compared to experimental measurements, and good overall agreement is found.

THEORETICAL CONSIDERATIONS

The Model and Analytical Results

Let us start by recapitulating the standard spin resonance experiment: a ferrite sample is placed inside an external constant (DC) magnetic field and is exposed to an alternating (AC) magnetic field oscillating at microwave frequencies. If the two magnetic fields are mutually perpendicular and if the frequency of the AC field is near the natural ferromagnetic resonance of the ferrite (determined by the DC field), an oscillating magnetic moment is induced in the sample precessing about the static field, and part of the microwave energy in the AC field is absorbed. The magnitude of the induced magnetization depends on the AC field strength and the susceptibility of the sample.

The dynamic susceptibility is generally described by a tensor quantity that relates two vectors to one another, the applied AC magnetic field $\mathbf{H}_{AC}$ and the resultant magnetization vector $\mathbf{M}$.

$$\mathbf{M} = \overleftrightarrow{\chi}\mathbf{H} \qquad [1]$$

In this study, only the diagonal entry of the susceptibility along the direction of the applied AC field will come into play. This quantity, which we call simply χ, measures the magnetic response of the sphere to an applied AC magnetic field along that field direction. Applying the Bloch equations to the ferromagnetic resonance, it can be shown (*12*) that the susceptibility takes the approximate form of

$$\begin{cases} \chi = \chi' - j\chi'', \text{ with} \\ \chi' = (\gamma M_0)\dfrac{T^2(\omega_0 - \omega)}{1 + T^2(\omega_0 - \omega)^2}, \text{ and} \\ \chi'' = (\gamma M_0)T\dfrac{1}{1 + T^2(\omega_0 - \omega)^2}. \end{cases} \qquad [2]$$

M_0 is the saturation magnetization and T is a phenomenological decay time. The more sophisticated Landau-Gilbert damping expression results in a slightly more complicated expression for the susceptibility (*13*) but is also phenomenological in nature. Here we choose the simpler form of Eq. [2].

Now consider the following modification to the standard spin resonance setup. In addition to the microwave excitation structure generating the alternating field at the sample, let us surround the sample with a copper loop terminated by a resistor, as shown in Fig. 1. It is apparent that the alternating field penetrates the loop structure as well as the ferrite crystal. Current will thus be induced in the terminated loop by the changing magnetic flux of the applied AC field and by the magnetic response of the ferrite. A detailed analysis of the resulting effect on the measured susceptibility of the system is given in the remainder of this section.

Applying Kirchhoff's loop rule to the loop in Fig. 1, it is apparent that

$$L\frac{di}{dt} + Ri = -\frac{d\Phi_m}{dt}, \qquad [3]$$

where the magnetic flux through the loop derives from the applied AC field and the magnetization of the crystal. Accordingly,

$$\Phi_m = \mu_0(A_l H + A_s M), \qquad [4]$$

where A_l and A_s refer to the loop area and cross-sectional sample area, respectively, H is the applied AC field, and M is the AC magnetization of the crystal. The second part of Eq. [4] is not exact but a good approximation.

The right-hand side of Eq. [3] can be thought of as a voltage driver giving rise to some current i in the

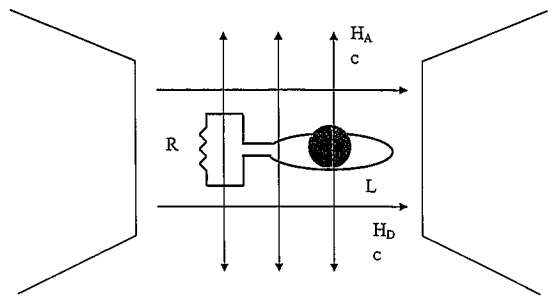

Figure 1 Basic schematic of the coupled ferromagnetic resonance model. The YIG sphere is exposed to both a DC and an AC field and surrounded by a loop of inductance L connected to a resistor R.

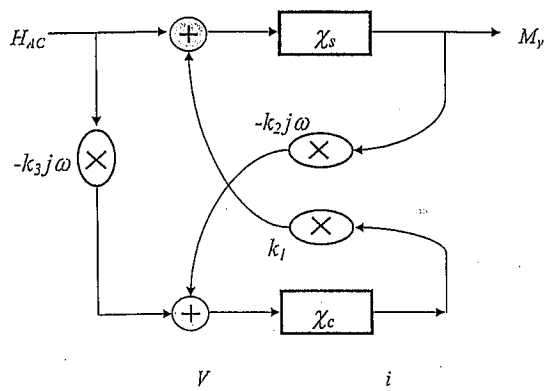

Figure 2 The diagrammatic feedback mechanism. An applied field H_{AC} enters on the left side and a certain magnetization M is induced on the right. The magnetization causes an *emf* in the loop, which drives a current i. This, in turn, creates a field at the YIG sphere.

loop. The current in the loop structure then is simply determined by the impedance of an RL circuit, via, $i = 1/Z\ V = \chi_c V$, with

$$\chi_c = \frac{R}{R^2 + (L\omega)^2} - j\frac{L\omega}{R^2 + (L\omega)^2}. \qquad [5]$$

Here, χ_c denotes the inverse impedance, or admittance, of the RL circuit of Fig. 1.

Qualitatively, we can describe the situation as follows: the applied magnetic field H produces an alternating magnetization in the sample, M, which induces an *emf* in the loop surrounding the sample. This *emf* then gives rise to an alternating current in the loop, which in turn produces a magnetic field at the sample. It is clear that this sequence of processes naturally lends itself to a feedback description.

The schematic diagram in Fig. 2 encapsulates the feedback mechanism. We start in the left upper corner, with an applied field, $H(t) = H(\omega)\, e^{j\omega t}$, producing a magnetization $M(t) = M(\omega)e^{j\omega t}$, where $M(\omega) = \chi_s H(\omega)$ is complex. By Eqs. [3] and [4], $M(t)$ produces a voltage, via

$$V_1(t) = -k_2 \frac{d}{dt} M(t), \text{ or } V_1(\omega) = -k_2 j\omega M(\omega). \qquad [6]$$

Comparison with Eq. [4] yields $k_2 = \mu_0 A_s = \mu_0 \pi r_s^2$. The other part of the voltage in the loop comes from the oscillating field $H(t)$ itself and yields $V_2(\omega) = -k_3 j\omega H(\omega)$, where $k_3 = \mu_0 A_l = \mu_0 \pi r_l^2$. Thus, the effective driving voltage is the sum of those two terms, $V(\omega) = V_1(\omega) + V_2(\omega)$, as indicated by the "+" sign in Fig. 2. The resultant current is given by $i(\omega) = \chi_c[V_1(\omega) + V_2(\omega)]$, which in turn will give rise to a magnetic field, $h(\omega) = k_1 i(\omega)$, with $k_1 = 1/2r_l$. This magnetic field $h(\omega)$ adds to the applied field $H(\omega)$, again indicated by the "+" symbol in the figure.

Following these steps in reverse, we can now write the magnetization as $M = \chi_s[H + h] = \chi_s[H + k_1 i] = \chi_s[H - k_1 j\omega\chi_c(k_3 H + k_2 M)]$. Collecting terms and solving for M yields the central equation,

$$\begin{cases} M(\omega) = \chi_{total} H(\omega), \text{ with} \\ \chi_{total} = \dfrac{\chi_s - j\omega k_1 k_3 \chi_s \chi_c}{1 + j\omega k_1 k_2 \chi_s \chi_c} \end{cases} \qquad [7]$$

Here, χ_{total} denotes the susceptibility of the combined system of ferrite sphere and loop structure. Equation [7] is the main analytic result of this article. In the next section, we use *Mathematica* (*14*) to plot this expression for realistic parameter values with no free parameters. In the experimental chapter of this book, these numerical results will be compared to experimental measurements.

Numerical Evaluation

To numerically evaluate χ_{total}, we first have to consider the constants appearing in Eq. [7]. The three geometric constants contained in χ_{total} are k_1k_2, k_1k_3, and L. The first one (k_1k_2) characterizes the mutual inductance of the coil and sample and can be approximated by $\pi/2\ \mu_0(r_s^2/r_l)$, although the actual value should be slightly higher. The second constant (k_1k_3) is exactly $\pi/2\ \mu_0 r_l$. The last constant (L) is the self-inductance of a simple loop and is given (*15*) by the approximation $\mu_0 r_l(\ln 8r_l/a - 2)$, where a denotes the radius of the copper wire (here ~0.14 mm).

The important constants characterizing the spin resonance are γM_0, ω_0, and T. The latter two are assigned the experimental values of 2π (3.49 GHz) and 300, respectively, to yield a Q-factor of around 6,600. M_0 is the saturation magnetization; for YIG, $4\pi M_0$ at room temperature is 1,750 G, and the gyromagnetic ratio γ is $1.76*10^7$ rad/*Oe* s (*6*). The radius of the YIG sphere, r_s is 0.45 mm in all experiments.

Figure 3(a) displays plots of χ_{total} for several different values of r_l, the loop radius, and R, the terminating resistance. The solid line at low frequencies corresponds to the intrinsic resonance of the YIG sphere with no surrounding loop present (i.e., where either $L = 0$ or $R \to \infty$). For the other traces, R was set to a small number (~0.1 Ω); the precise value is not crucial here. The dotted trace to somewhat higher

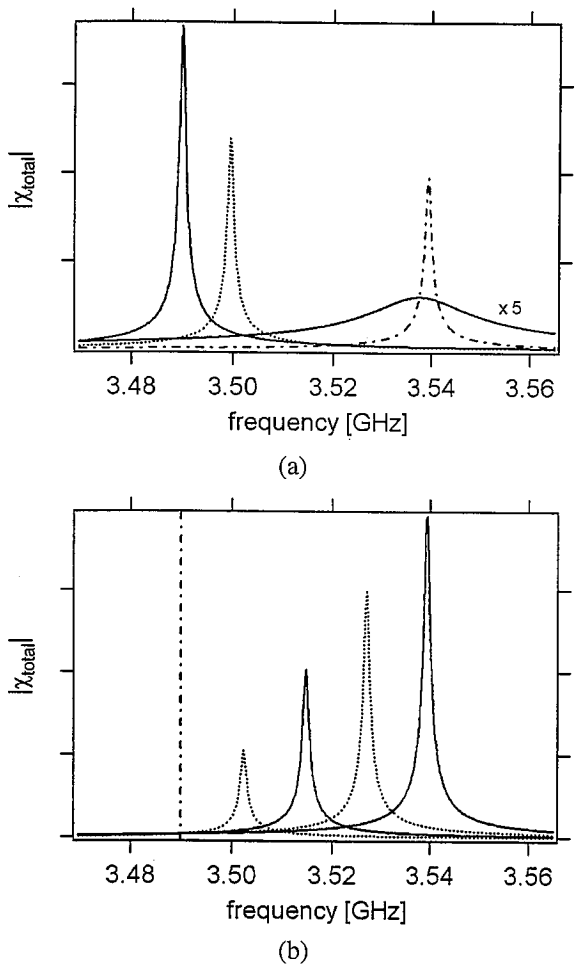

Figure 3 (a) The coupled susceptibility curves for different values of the circuit parameters. The left (solid) line depicts the uncoupled (intrinsic) resonance, the dotted line is for a loop radius of 1.75 mm and small resistance, and the dot-dashed line is for a loop radius of 0.825 mm. The broad solid line represents the resistive case ($R = 17\ \Omega$). (b) The coupled susceptibility for different values of the saturation magnetization of the sample. The dashed vertical line indicates the uncoupled resonance frequency. The curves are for different values of γM_0, starting from 2.45/4 and increasing in equal steps to 2.45.

frequency represents the YIG sphere with a loop of radius 1.75 mm around it. In the dot-dashed trace, the loop radius was decreased to 0.825 mm. Finally, the solid line is for a loop of the same radius, 0.825 mm, but now terminated by a 17 Ω resistor. Since some energy can now be dissipated in the resistor, the width of the response curve is seen to significantly increase. As the resistance is further increased, the resonance line continuously shifts to lower frequencies, approaching ω_0 (from above) at very large values of R. The main point, however, is that the coupling to the coil has the effect of shifting the ferromagnetic resonance to higher frequencies for all parameter values.

In Fig. 3(b), the loop radius is fixed at 0.825 mm, but the value of M_0 is varied. The leftmost trace corresponds to $\gamma M_0 = 2.45/4$; its value is then incremented by this value up to 2.45 in the subsequent traces to the right. The dashed vertical line indicates the position of the uncoupled YIG resonance. The frequency shift induced by the coil is seen to increase linearly with M_0.

The main qualitative results from the numerical evaluation of the analytical χ_{total} can be summarized as follows: (1) The resonance line shifts to higher frequencies when the YIG sphere is coupled to an LR circuit; (2) The shift is a monotonically decreasing function of coil radius and is surprisingly insensitive to the number of turns of the coil; (3) A terminating resistor acts to broaden the line and to shift the frequency somewhat lower relative to the closed loop resonance line; and (4) The shift in resonance frequency is strongly dependent on the saturation magnetization M_0 determining the maximum AC susceptibility of the magnetic mode. As expected, the larger the M_0, the larger the resultant frequency shifts.

EXPERIMENTAL DATA

The Experimental Setup

Figure 4 illustrates the basic experimental setup. The local oscillator output of the spectrum analyzer is mixed with a fixed frequency microwave signal to produce the probe signal. The mixing stage ensures that the probe signal is swept in synchrony with the center frequency of the spectrum analyzer, and it effectively turns it into a scalar network analyzer. This signal is transmitted via SMA coaxial cables and passes through the nonresonant excitation structure patterned on a PC board. It consists of a microstrip line on both ends bent around in the shape of a circular loop of radius 4 mm at the center. The YIG sphere is placed on the PC board dielectric inside this loop structure, which produces the AC magnetic field exciting the ferromagnetic resonance. The microwave signal transmitted through this system then enters the spectrum analyzer for detection. The resultant spectrum displayed on the spectrum analyzer screen is sent to a digitizing oscilloscope and transmitted to the computer via GPIB cables. In this setup, it is easy to place an external coil, either closed or attached to a coaxial cable, around the YIG sphere. One can descend the coil from above toward the sample and, for maximum coupling strength, the coil can simply rest on the PC board around the YIG sphere. Care has to be taken to center the coil with respect to the sample.

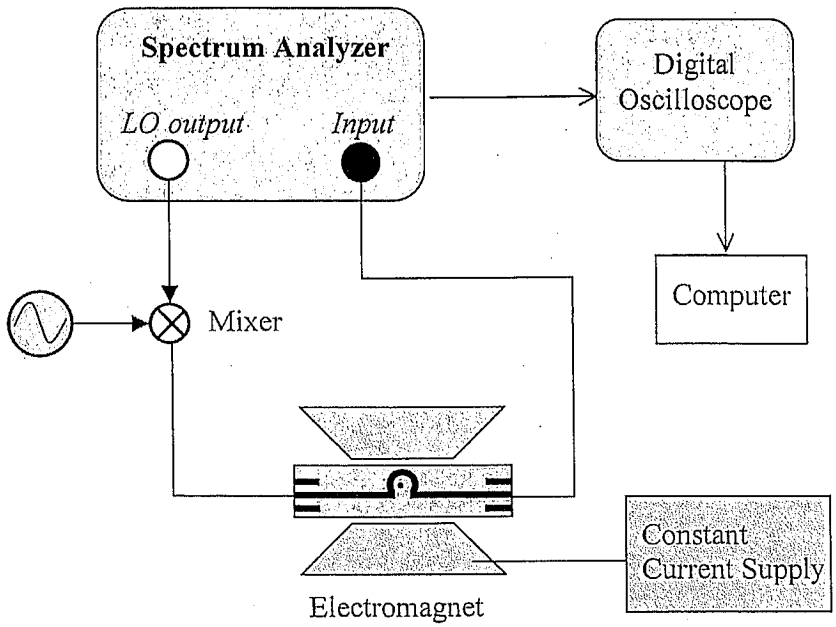

Figure 4 The experimental setup. The local oscillator output of a spectrum analyzer is used to excite the ferromagnetic resonance of the YIG sphere placed in a patterned PC-board loop structure. The transmitted microwave signal is detected by the spectrum analyzer and sent to a digital oscilloscope.

Within the framework of the theoretical model outlined in the previous section, the larger excitation loop on the PC board provides the alternating field probing the resonance, whereas the removable outside coil represents the external coupling structure. In the model the excitation loop is not included because the origin of the alternating field is not specified. Thus, one simplifying (but somewhat crude) approximation is made when comparing theory and experiment, namely that the applied field generated by the PC board loop is not affected by currents in the external coil. It is clear that this cannot be exactly true, as the two are coupled via their mutual inductance. It can be shown that when the excitation loop is explicitly included in the model, the complexity of the feedback diagram quickly grows. As demonstrated in the next section, however, this simple model is already successful in describing many of the observations.

Measurement Results

We now compare each of the four predictions listed at the end of the theory section with experimental data. Figure 5(a) shows the transmission spectra for the isolated YIG sphere and the YIG sphere surrounded by closed coils of two different radii, 1.75 mm and 0.825 mm, respectively. The applied field was set to about 1200 *G* so as to shift the resonance to 3.49 GHz, where it is characterized by a small line-width (~1 MHz). The observed upward frequency shifts of 7.8 MHz and 44.6 MHz and their ratio are close to the values predicted by our model, as seen in Table 1 below. The difference arises most likely from the uncertainty in the values of some experimental parameters. In further agreement with the model, it is shown experimentally that the number of turns in the coil has no measurable effect on the frequency shift. Incidentally, this coupling provides a means to tune the resonance frequency of YIG very finely by simply varying the height of the coil above the YIG sphere.

We next examine the case where the leads of an open coil are connected to a coaxial cable that is terminated at the other end with a 50 Ω resistor. This method is the easiest way of attaching a resistor to the coil inductor. The value of 50 Ω is chosen because it matches the impedance of the coaxial cable and therefore produces no reflections that would modify the effective impedance as seen from the coil (2). The effect of the resistor is illustrated in Fig. 5(b). Here, the low-frequency line is again the uncoupled ferromagnetic resonance; the sharp line to the right is obtained by placing a closed coil around the sample. The broad line corresponds to an open coil of the same diameter as the closed one connected to a 50 Ω resistor via a coaxial cable. The dramatic reduction of the effective Q-factor is apparent. Qualitatively

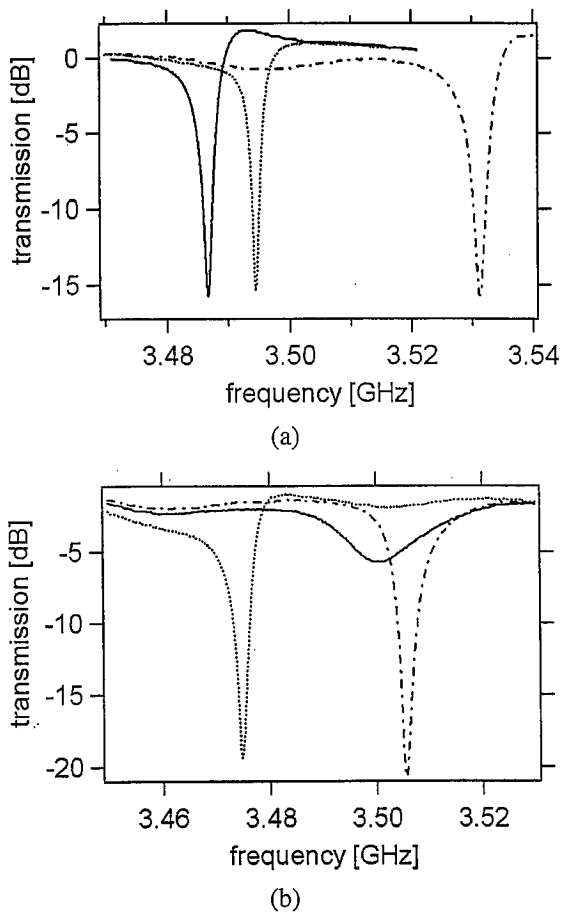

Figure 5 (a) Experimental transmission lines for a YIG sphere surrounded by a simple copper loop. The solid line (left) gives the result without the presence of a loop, the dotted line is for the larger loop (1.75 mm radius), and the dot-dashed line is for the smaller loop (0.825 mm). (b) The effect of adding a resistor. The dotted line is the uncoupled resonance, the dot-dashed line (right) corresponds to the YIG surrounded by a loop, and for the solid line a 50 Ω resistor was added. This was done by attaching the loop to a terminated coax-cable.

speaking, it arises because another pathway for the dissipation of energy in the magnetic mode has opened up, namely via electrical dissipation at the resistor. Comparing Figs. 3(a) and 5(b) we find qualitative agreement between experiment and theory; both the predicted broadening and the small red-shift are observed. However, for a quantitative match the excitation loop has to be included in the analysis.

In another test of the model, we now turn to the influence of the intrinsic properties of the magnetic resonance on the shift in the coupled resonance frequency. For this purpose, we can substitute the pure YIG sphere considered so far (r_s = 0.45 mm) with a slightly smaller Gá:YIG sphere of radius r_s = 0.41 mm. When doping YIG with Ga, the nonmagnetic gallium ions replace some of the iron ions, thus reducing the saturation magnetization M_0 of the crystal. For a 20% doped crystal, ($Y_3Fe_{4.05}Ga_{0.95}O_{12}$), M_0 is reduced from 141.6 kA/m to 31.8 kA/m (*1*). Reducing γM_0 by this ratio, we can compare the measured shift for the Ga:YIG resonance with the model predictions.

Table 1
Predicted and Measured Renormalized Frequency Shifts

	Model	Experiment
Resonance shift for YIG		
r_l = 1.71 mm	9.4MHz	7.8MHz
r_l = 0.83 mm	49.0MHz	44.6MHz
Ratio	5.2	5.7
Resonance shift for Ga: YIG (r_l = 0.83 mm)	8.7MHz	7.4MHz
Ratio (YIG/Ga:YIG)	5.6	6.0

Figure 6 shows the ferromagnetic resonance of Ga:YIG. The DC magnetic field was chosen to place the Ga:YIG resonance near the prior resonance frequency, at 3.5 GHz. The dotted line displays the uncoupled resonance, the dot-dashed line the resultant resonance with the 1.75 mm radius coil, and the solid line the resonance with the 0.825 mm radius coil surrounding the sample. Note that the decrease in absorbed power (the y-axis scale) relative to the measurements on the pure YIG sphere also indicates the lower experimental coupling. In fairly good accord with theory (see Table 1), the frequency shift attained

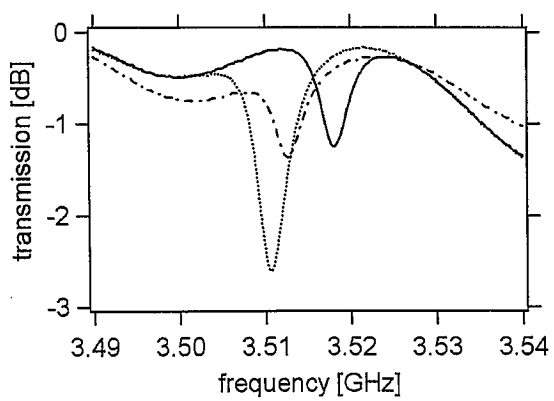

Figure 6 The transmission lines for the Ga:YIG sphere of slightly smaller diameter. The lines again correspond to no loop, large and small loop, respectively. Notice that the frequency shifts are all reduced by a large factor due to the decreased magnetization of the sphere.

with the smaller coil decreases from 44.6 MHz for the pure YIG sphere to 7.4 MHz, a ratio of 6.

Another way of modifying the effective magnetic moment involved in the resonance is to examine a different magnetostatic mode from the uniform ferromagnetic resonance. Such magnetostatic modes represent additional solutions to the boundary value problem of the magnetized ferrite sphere in vacuum and are characterized by a spatial dependence of the magnetization vector inside the sample. The excitation of magnetostatic modes (other than the uniform mode) usually requires a spatially nonuniform AC magnetic field. In the stripline coupling scheme employed here, such nonuniformity can best be achieved by simply drilling a small hole into a straight microstrip line and placing the YIG sphere in it (*1*). This geometry will strongly couple to a particular magnetostatic mode, the (2,1,1) mode, the resonance of which appears at significantly lower frequency (or higher DC fields at the same frequency). Using such a coupling structure, the magnetostatic mode was clearly identified in the transmission spectrum as an absorption line of 7 dB depth at 3.02 GHz.

Despite this strong coupling, no frequency shift was observed upon placement of a closed coil around the sample for all but the smallest coil radii. It should be emphasized that this experiment really goes beyond the applicability of our model. The simple addition of the current-induced field to the external field, as prescribed by the model (see Fig. 2), is no longer valid as the applied AC field is now spatially nonuniform.

Nevertheless, this null result seems intuitively reasonable as the magnetostatic mode carries no net magnetic moment, which is the source of the feedback mechanism described. Only for the smallest loop radii could a resonance-frequency shift be discerned. For a loop radius of 0.825 mm, a shift of 1.5 MHz at 3.02 GHz was measured, which is less than the line width of about 2 MHz.

CONCLUSION

We have shown experimentally that by coupling the uniform magnetic mode of a ferrite to an LR circuit, the resonance frequency of the combined system moves higher. Because this coupling mechanism acts only on the uniform ferromagnetic resonance, it adjusts the position of the uniform mode relative to the magnetostatic and spin-wave spectrum.

We have characterized the resonance shifts in terms of both the circuit parameters (L and R) and the spin parameter (M_0). The observed frequency shifts are in good agreement with the feedback model we have developed. In particular, we find that the simple experimental procedure described here can be used to ascertain M_0 and thereby the magnitude of the diagonal element of the susceptibility tensor.

The off-diagonal element may in principle be accessible as well via a simple modification of the experiment. Instead of aligning the external coil along the direction of the AC field, it is rotated by 90° so that it is sensitive to the perpendicular component of the magnetization. Here the excitation and probe coils are decoupled, but the associated magnetic field now have to be added as vectors, necessitating a reformulation of the theoretical model.

ACKNOWLEDGMENTS

The authors thank A.J. Sievers at Cornell University for providing the YIG samples and A. J. Sievers and M. Sato for many helpful discussions.

REFERENCES

1. Helszajn J. 1985. YIG resonators and filters. New York: John Wiley & Sons.
2. Pozar DM. 1988. Microwave engineering. 2nd ed. Singapore: John Wiley & Sons.
3. Walker LR. 1957. Magnetostatic modes in ferromagnetic resonance. Phys Rev 105:390–399.
4. Dillon JF. 1958. Magnetostatic modes in ferrimagnetic spheres. Phys Rev 112:59–63.
5. Suhl H. 1957. The theory of ferromagnetic resonance at high signal powers. J Phys Chem Solids 1:209–227.
6. Kovshikov NG, Kalinikov BA, Patton CE, Wright ES, Nash JM. 1996. Formation, propagation, reflection, and collision of microwave envelope solitons in yttrium iron garnet films. Phys Rev B 54:15210–15223.
7. Poole CP. 1996. Electron spin resonance. 2nd ed. New York: Dover.
8. Silber L. 1963. Intrinsic properties of ferrites. In: Sucher M, Fox J, editors. Handbook of microwave measurements, vol. 2. New York: Polytechnic Press.
9. Artman JA, Tannenwald PE. 1955. Measurement of susceptibility tensor in ferrites. J Appl Phys 126:1124–1132.
10. Carter PS. 1961. Magnetically-tunable microwave filters using single-crystal yttrium-iron-garnet resonantors. IEEE Trans MTT 9:252–260.
11. Moll NJ. 1977. Coupling of circuit structures to magnetostatic modes of ferromagnetic resonators. IEEE Trans MTT 25:933–938.
12. Bloombergen N. 1950. On the ferromagnetic resonance in nickel and supermalloy. Phys Rev 78:572–580.
13. Morrish AH. 2003. The physical principles of magnetism. New York: IEEE Press Classic Reissue.
14. Wolfram Research. 1999. Mathematica 4. Champaign, IL: Wolfram Research.
15. Ramo S, Whinnery JR. 1953. Fields and waves in modern radio. New York: John Wiley & Sons.